

Using Magma Mixing/Mingling Evidence for Understanding Magmatic Evolution at Mount Bidkhan Stratovolcano (South-East Iran)

S. Khalili Mobarhan^{1,2,*} and H. Ahmadipour¹

¹*Department of Geology, Faculty of Science, Shahid Bahonar University
of Kerman, Kerman, Islamic Republic of Iran*

²*Department of Geology, Faculty of Science, Payame Noor University, Kerman, Islamic Republic of Iran*

Received: 23 September 2009 / Revised: 15 May 2010 / Accepted: 4 June 2010

Abstract

Mount Bidkhan stratovolcano is located in the central Iranian volcanic belt. It is composed of several types of pyroclastic deposits, lava flows and intrusive bodies. Textural and chemical characteristics of plagioclase phenocrysts from the eruptive products volcanic edifice, record complex magma mixing events over the lifetime of the volcano. Evidences such as xenocrystic high Al+Ti clinopyroxene and calcic cored plagioclase phenocrysts (An 75) in andesites, sieve-textured, dusty, and oscillatory zoned plagioclase together with clear normally zoned ones in the same sample and the wide compositional range of the plagioclase rims, show that magma mixing events have been playing an important role in the origin of Bidkhan eruptive products. Based on whole evidences, we propose a model for the evolution of Bidkhan parent magmas. According to the model, it is likely that mantle derived basic melts are injected into the lower crust, cause partial melting and produced acidic primitive melts. These two melts are then, mixed and resulted hybrid magmas, ascend toward the shallower reservoirs. Repeated magma injection gives rise to a second mixing event. Thus eruptive products at Mount Bidkhan have been originated from the mixing of intermediate hybrid magmas within shallow magma chambers. Sometimes, two melts have been erupted simultaneously as mingled melts. This model can be tested for other volcanic province of central Iranian volcanic belt.

Keywords: Central Iranian volcanic belt; Magma mixing; Mingling; Mount Bidkhan; Oscillatory zoning

Introduction

According to definitions of Bacon [4] and Sparks and Marshal [30], mixed magmas that are blended to form a

homogenous composition are termed "mixed" or "hybrid" magmas [21], whereas, the term "mingling" or "comingling" is used if magmas are heterogeneous physical mixtures at a microscopic or mesoscopic scale

* Corresponding author, Tel.: +98(913)3414410, Fax: +98(341)3342791, E-mail: khalilishahram@pnu.ac.ir

(like banding or enclave/inclusions are in the rock). In this study, we use these terms for the same phenomena in Bidkhan eruption products.

This study is aimed at understanding of magma mixing events in Bidkhan stratovolcano magmas and petrogenesis of related volcanics by evaluating various data. For this goal, we present detailed petrographic, mineralogical and geochemical description of the Bidkhan products to investigate the pre-eruptive history of the magmas and then we develop a generalized model for the evolution of magmas at Bidkhan.

Magma mixing is a fundamental and effective process in the evolution of Iranian intermediate-silicic volcanic rocks. Many Iranian Cenozoic volcanic edifices shows various disequilibrium textured phenocrysts that have been produced by magma mixing [9], and Bidkhan stratovolcano is one of them that shows plenty of evidences for magma mixing and mingling.

Many studies have demonstrated the complexity of intermediate magma chambers (like in Bidkhan), a complexity that is related to magma composition, fractional crystallization, assimilation and magma mixing. Moreover, compositional diversity in erupted products and disequilibrium textures in phenocrysts have been attributed to magma mixing at numerous arc calcalkaline related volcanoes (e.g. [33], [22]).

There is now a consensus that magma mixing effectively occurs in replenished magma chambers and during eruptions; Therefore, [10] some studies have concentrated on the physical mechanisms and dynamics of magma mixing [30]. The triggering of explosive eruptions by magma injection and subsequent mixing has also been proposed at several volcanic centers (e.g. Askja by Sparks et al. [31], and Pinatubo by Eichelberger and Izbekov, [8]). This process reflects in both bulk composition and phenocryst assemblage. Plagioclase crystals record crystallization and magma mixing of their host magma, because of slow diffusion of alkali elements in feldspar compared with the time scale of magmatic events. In calcalkaline magmatic systems, compositional variations in feldspar have been used to interpret variations in the physical and chemical conditions brought about by processes such as magma mixing, pressure changes and convection during crystallization (e.g. [25]).

Materials and Methods

Whole rock chemical analyses for major elements were performed by X-ray fluorescence spectrometry at the Dipartimento di Scienze Geologiche of the University of Catania (Italy) by means of a Philips

PW2404 WD-XRF on powder pellets, correcting the matrix effects according to Franzini et al. [13]. FeO concentrations were obtained by classic KMnO_4 titration; loss of ignition (L.O.I.), corrected for Fe^{2+} oxidation, was determined by gravimetric methods and commonly is ~ 1.5 wt%, implying that sampled rocks were not significantly weathered. Trace and rare earth elements were determined by ICP-MS at the SGS Laboratories of Toronto

(Ontario, Canada). Powdered rock samples were fused by Na-peroxide in graphite crucibles and dissolved using dilute HNO_3 . Fusion process involved the complete dissolution of samples in a molten flux. Trace element analyses were then made by means of a Perkin Elmer ELAN 6100 inductively coupled plasma mass spectrometer. Four calibration runs were performed on international certified reference materials (USGS GXR-1, GXR-2, GXR-4 and GXR-6) at the beginning and end of each batch of 15 samples. Precision is better than $\sim 7\%$ for all trace elements. The major element composition of crystals was analyzed by using the electron microprobe at Dipartimento di Scienze Geologiche of Catania by means of a TESCAN-VEGA\LMU scanning electron microscope (SEM) equipped with an EDAX XM4 60 microanalysis working in energy dispersive spectrometry (EDS). Operating conditions were 20 keV accelerating voltage and 0.2 nA beam current. The accuracy is $\sim 0.5\%$ for abundances >15 wt%, $\sim 1\%$ for abundances around 5 wt% and $\sim 20\%$ for abundances around 0.5 wt%. The precision is better than 1% for SiO_2 , Al_2O_3 , FeO, MgO and CaO and better than 3% for TiO_2 , MnO, Na_2O , K_2O and P_2O_5 . Plagioclase and clinopyroxene phenocrysts were analyzed in detail along core-rim transects with regular steps ranging between 10 and 30 μm , depending on the presence of textures, fractures and inclusions along the profile.

Geological Framework and Field Observations

Bidkhan stratovolcano has erupted in the South-East edge of Central Iranian Volcanic Belt (Urmieh-Dokhtar volcanic belt), just to the south of Bardsir town in the Kerman province. This volcanic edifice, 3500 m high, is underlain by Eocene, Oligocene volcanic basement (in some parts by Miocene rocks) and composed of several lava flows, different types of pyroclastic deposits, dykes and plugs (Fig. 1).

According to Dimitrijevic [7], this volcano belongs to a series of Plio- Pleistocene volcanoes (Mosahim, (2.6 ma. by HasanZadeh, [16]), Aj-e Bala and Aj-e Paaïn) whose location is controlled by northwest-southeast trending faults.

block and ash pyroclastic flows (Fig. 3d). They evenly mantle the original topography of the edifice.

There are some dacitic dykes and plugs (Fig. 3e) that have been injected into the central and proximal areas and are related to the final Bidkhan magmatic activities.

Evidence for magma mingling commonly occurs in Bidkhan lava flows as centimeter sized darker and folded bands between lighter ones, with irregular boundaries (Fig. 3f). Lithologically, these two parts are fairly similar and their different appearances are due to different groundmass colors.

Petrography

Bidkhan volcanic products are generally non-to slightly vesicular, porphyritic to partially glomeroporphyritic lavas and dykes ranging between andesite to dacite compositions. Typical phenocryst assemblages

are: andesites: Plg+Cpx+Opx±Amph±Fe-Ti oxides, dacites: Plg+Amph+Bio±Cpx±Opx±Qz+Fe-Ti oxides.

All lithologies are crystal rich, averaging between 40-50% crystal by volume with plagioclase as dominant phenocryst and micro phenocryst phase. Other minerals may be present in varying amounts. These phases are set in the groundmass composed of glass and microlitic plagioclase. Plagioclase is the most abundant mineral in Bidkhan rocks.

In all bulk-rock compositions, plagioclase occurs as large (up to 5 mm) euhedral to subhedral phenocrysts in isolation or in glomerocrysts and as equant microphenocrysts (100-300 μm in diameter) and lath-shaped microlites (<100 μm) in the groundmass. Clinopyroxene occurs in andesites as isolated euhedral to subhedral phenocrysts up to 2 mm across, and as rounded glomerocrystic aggregates. Orthopyroxene occurs as individual subhedral to euhedral lath-shaped microphenocrysts (<0.5 mm across). Pyroxene compositions are typical of calcalkaline rock series [11]. Clinopyroxene (Wo 42 En 44 Fs 14) are mainly augite and Orthopyroxene are hypersthene (Wo 2 En 72 Fs 26).

Amphibole is present in more silica rich rocks of Bidkhan as brown-green prismatic phenocrysts ranging in size up to 5 mm. In some cases, amphibole is rimmed by opaque minerals, presumably as a result of breakdown during decompression [12]. Biotite is sometimes found in the dacitic dykes and plugs (<2 vol %) and occurs as euhedral single medium sized phenocrysts (up to 3 mm across). Quartz typically accounts for 1-2 vol % of dacitic rocks and is always found large rounded and/or irregularly embayed phenocrysts.

Various Types of Plagioclases Based on Petrography

Plagioclase crystals found in Bidkhan rocks, fall into two populations based on texture.

The first population are those plagioclases that show disequilibrium textures such as sieved, dusty, fritted, honeycomb, riddle, spongy [36], cellular intergrowth [2], patchy [15] and different types of oscillatory zoning. Both phenocrysts and micro phenocrysts may show one or more of these textures. Second population of plagioclase crystals in Bidkhan rocks are clear type phenocrysts, microphenocrysts and microlites are represent equilibrium texture for the phases (Fig. 4). The most common type (75 vol %) consists of large grains (up to 1 cm in length) with normal oscillatory zoned (Fig. 4). The second less common plagioclase consists of grains with a coarsely sieved interior. Resorption zones surround the interior of oscillatory and coarsely sieved ones (Fig. 4).

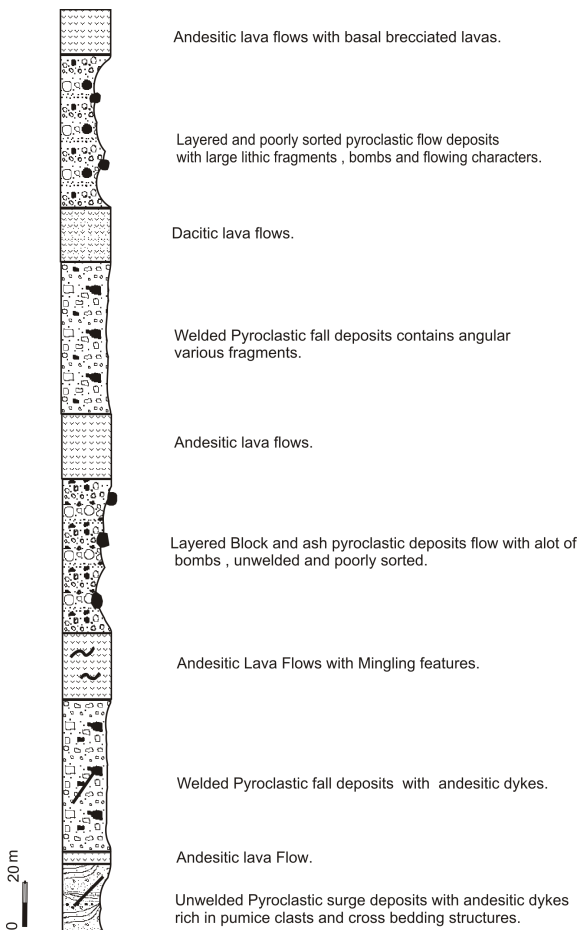


Figure 2. generalized volcano-stratigraphic column of Bidkhan volcanic products in caldera walls.

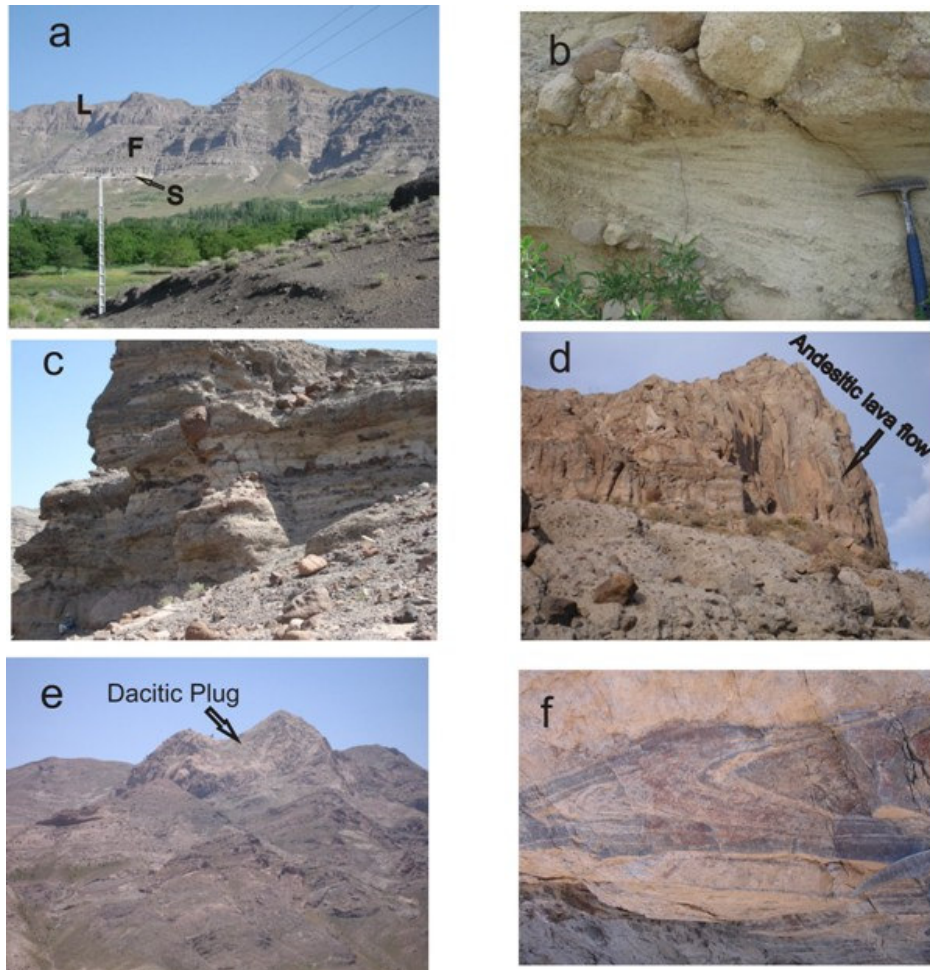


Figure 3. a) Bidkhan volcanic products' pile, with white colored pyroclastic surge in the base (S), pyroclastic flows in middle (F), and lava flows at the top (L), b) close up view of pyroclastic surge deposits contain cross-bedding structure, c) Bidkhan pyroclastic flow deposits, d) Bidkhan andesitic blocky lava flow, e) Dacitic plug that has cut proximal facies volcanic products, f) Mingling structure in Bidkhan lava flows.

The coarse sieved texture is due to the presence of abundant melt inclusions, which vary from circular to elongate and irregular shapes. The high concentrations of inclusions suggest that they form a system of interconnected channels permeating the crystals' interior [17]. Some of the plagioclase crystals show complex internal zoning with irregular zone boundaries characterized by rounded corners and lobate embayments (Fig. 4) and sometimes are overgrown by euhedral outer crystal zones (Fig. 4). These textures, with resorbed and embayed plagioclase faces called "partial-dissolution surfaces" by Tsuchiyama [36].

Other disequilibrium textures in Bidkhan plagioclase crystals such as dusty and patchy are shown in Figure 4.

Some of disequilibrium textures are seen in microphe-nocrysts (Fig. 4). In Figure 4 clear type of plagioclase phenocrysts, microphe-nocrysts and microlites are also shown.

Whole Rock Geochemistry

Whole rock major and trace element contents for representative Bidkhan samples are listed in Tables 1, 2 and 3. According to the classification schemes of Pecerrillo and Taylor [26] and Le Maitre [20], Bidkhan rocks form a medium to high K calc-alkaline suit ranging in composition from andesite to dacite (Fig. 5a and 5b).

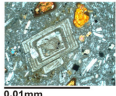
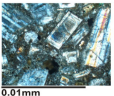
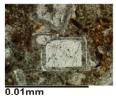
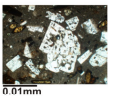
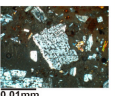
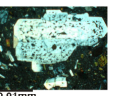
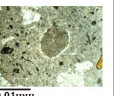
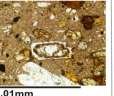
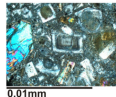
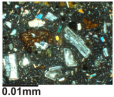
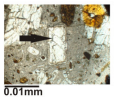
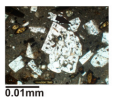
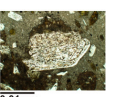
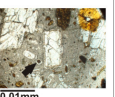
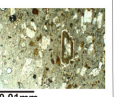
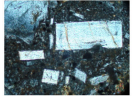
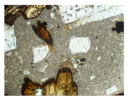
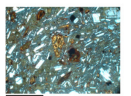
Disequilibrium textures in plagioclase phenocrysts	Oscillatory zoned plagioclase			Sieved plagioclase				
	Normal oscillatory zoned plagioclase	Oscillatory zoned with resorption rim	Oscillatory zoned with clear thin rim	Coarsely sieved	Coarsely sieved with resorption rim	Sieved with clear rim	Dusty	Patchy
								
An mol% in core	67	28	32	34	61	61	44	56
Disequilibrium textures in plagioclase microphenocrysts					No image			
An mol% in core	51	49	48	50		47	32	41
Equilibrium textures in plagioclase phenocrysts	clear normal zoned plagioclase		Equilibrium textures in plagioclase micro phenocrysts	clear normal zoned plagioclase		Microlites	clear normal zoned plagioclase	
								
An mol% in core	44		An mol% in core	55		An mol%	45	

Figure 4. Photomicrographs of texturally types of plagioclases in Bidkhan eruptive products and their An mol% in the cores.

Many of compositional arrays of Bidkhan samples are linear (e.g. Fe, Ca, Y (Fig. 5 c, d, i)) which support a magmatic differentiation in parental magmas. Some element arrays, however, are scattered (e.g. Ba, Sr, P (j, h, g)) or curvilinear (e.g. Al, Na (e, f)). These suggest that processes such as crystallization, and assimilation also probably operate in the magma chamber. In addition, some features such as high amounts of Th/Nb and Zr/Nb ratios in Bidkhan samples (Tables 1, 2, 3), suggest crustal contamination in the genesis of the magma.

Whole rock compositional range in our samples is narrow from 59 to 65 wt% for SiO₂ and variation diagrams show a short range differentiation between andesitic to dacitic melts. This means, in Bidkhan, intermediate magmas have differentiated in a short compositional range in magma chamber. The whole rock data have tested and plotted in several well known magma mixing indication diagrams (e.g. [5], [10], [18] and [35]), but there are not any magma mixing indication between basaltic and dacitic melts in those diagrams. This means that if there were mixing events between basic and acidic melts they have not reflected in the whole rock compositions of Bidkhan eruption products. In fact these diagrams just show a continues short range differentiation. These results are confirmed by field and petrographic observations, because we have not any basaltic eruption or basic enclaves or basaltic bands in the field. So, field observations and whole rock

chemistry for Bidkhan rocks suggest that the last melts that have differentiated and erupted from shallow magma chambers had been intermediate (probably andesitic) melts and have been repeatedly invaded by newly intermediate batches of magmas during differentiation.

Then we have to search the traces of magma mixing in mineral chemistry, especially plagioclase crystals in the Bidkhan rocks.

Plagioclase Chemistry

Microprobe analysis of cores, middle and rims of Bidkhan plagioclase crystals are listed in Table 4. Because different rock types in Bidkhan are relatives (Fig. 5a) and for understanding correlation between plagioclase crystals and whole rock compositions, we grouped the rocks into dacites, andesites and transitional rocks based on composition and according to TAS diagram (Fig. 5a).

As shown in Figure 6 and Table 5, core compositions of plagioclase phenocrysts range from 28-72 and rims are slightly more sodic, however some of them have a little orthoclase component (Figure 6). But in general, there are not any clear distinctions between different rock types in this regard.

In Table 5 An mol% ranges have shown for the plagioclase phenocrysts cores. In andesites, those plagioclase cores with An 50-56 are in the most

Table 1. Whole-rock compositions of lithics in pyroclastic deposits (Selected from 13 samples) Major oxides were determined by XRF, the others by ICP-MS

Sample	K2	K7	O6	F9	B9	F1
<i>Wt %</i>						
SiO ₂	64.71	60.06	62.22	62.99	63.02	60.63
TiO ₂	0.58	0.60	0.49	0.50	0.57	0.70
Al ₂ O ₃	17.48	16.70	16.37	17.23	16.98	17.28
Fe ₂ O ₃	3.68	4.51	3.13	2.70	3.94	5.70
FeO	0.68	1.02	1.55	1.68	1.08	0.70
MnO	0.01	0.10	0.10	0.08	0.08	0.06
MgO	0.38	2.26	2.21	1.21	1.59	1.23
CaO	4.25	5.88	5.19	4.48	5.13	5.21
Na ₂ O	4.03	4.19	3.64	3.79	4.11	4.28
K ₂ O	2.16	2.57	2.75	3.16	2.62	2.08
P ₂ O ₅	0.16	0.30	0.20	0.17	0.19	0.20
L.O.I.	1.87	1.81	2.16	2.00	0.68	1.92
Total	100.00	100.00	99.99	100.00	100.00	100.00
FeOtot	3.99	5.08	4.36	4.12	4.63	5.83
<i>ppm</i>						
Ba			519		533	492
Be			0		0	0
Cr			20		20	80
Cu			26		40	30
Li			0		10	0
Mn			680		550	390
Ni			18		13	36
Sc			6		5	5
Sr			646		725	680
V			99		96	100
Zn			72		68	56
Ag			0		0	0
As			0		0	0
Bi			0		0	0
Cd			0		0	0
Ce			61.7		61.1	60.6
Co			16.8		15	18.6
Cs			6.9		5	2.5
Dy			2.07		2.03	2.07
Er			1.17		1.05	1.04
Eu			1.15		1.31	1.26
Ga			18		20	21
Gd			3.18		3.44	3.23
Ge			2		1	1
Hf			4		4	4
Ho			0.43		0.38	0.43
In			0		0	0
La			44		41	40.6
Lu			0.2		0.15	0.14
Mo			3		2	0
Nb			8		7	8
Nd			27.9		29.6	28.9
Pb			16		13	11
Pr			7.96		8.2	7.95
Rb			95.8		78.6	69.2
Sb			0.8		0.6	0.5
Sm			4.2		4.8	4.4
Sn			2		2	1
Ta			0		0	0
Tb			0.47		0.47	0.49
Th			20.9		13.9	16.3
Tl			0.6		0	0
Tm			0.17		0.13	0.14
U			4.55		3.5	3.43
W			2		1	1
Y			12.4		10.9	11.5
Yb			1.1		0.9	1
Zr			149		134	123

Table 2. Whole-rock compositions of dykes (Selected from 13 samples) Major oxides were determined by XRF, the others by ICP-MS

Sample	Q10-1	V2	X4	D7	V1	D3
<i>Wt%</i>						
SiO ₂	66.26	63.54	66.29	64.78	59.00	64.94
TiO ₂	0.46	0.51	0.46	0.49	0.71	0.56
Al ₂ O ₃	16.74	16.68	15.58	16.50	17.60	16.76
Fe ₂ O ₃	3.35	3.62	3.20	2.66	3.92	3.35
FeO	0.41	0.90	0.76	0.90	1.46	0.67
MnO	0.04	0.08	0.05	0.04	0.07	0.04
MgO	0.89	1.48	1.24	1.18	2.04	1.17
CaO	3.80	4.75	3.78	4.55	6.50	4.08
Na ₂ O	4.28	4.01	3.82	4.00	4.17	3.99
K ₂ O	2.37	2.93	2.71	2.47	2.28	2.54
P ₂ O ₅	0.15	0.17	0.14	0.17	0.28	0.19
L.O.I.	1.26	1.30	1.97	2.25	1.97	1.71
Total	100.00	100.00	100.00	100.00	100.00	100.00
FeOtot	3.43	4.16	3.64	3.30	4.99	3.69
<i>ppm</i>						
Ba			511			478
Be			0			0
Cr			20			0
Cu			26			57
Li			20			30
Mn			400			280
Ni			13			14
Sc			0			0
Sr			513			578
V			73			84
Zn			63			74
Ag			0			0
As			0			0
Bi			0.1			0
Cd			0			4.1
Ce			36.8			39.8
Co			12.1			12.4
Cs			3.4			3.8
Dy			1.19			1.21
Er			0.61			0.64
Eu			0.89			0.97
Ga			17			18
Gd			2.18			2.36
Ge			1			1
Hf			3			3
Ho			0.23			0.24
In			0			0
La			25.4			26.3
Lu			0.07			0.08
Mo			0			0
Nb			6			5
Nd			18.1			19.9
Pb			9			8
Pr			5.15			5.51
Rb			76.3			66.6
Sb			0.9			0.7
Sm			3			3.4
Sn			1			1
Ta			0			0
Tb			0.29			0.31
Th			10.5			7.8
Tl			0			0
Tm			0.07			0.07
U			2.9			2.63
W			1			1
Y			6.7			6.7
Yb			0.5			0.5
Zr			85.4			91.4

Table 3. Whole-rock compositions of lavas (selected from 23 samples) Major oxides were determined by XRF, the others by ICP-MS

Sample	R5	Q8	R8	B3	P5	D9	V4	G7	L6	B12	V8	N1	An
<i>Wt%</i>													
SiO ₂	59.52	63.52	59.92	62.42	60.56	65.21	61.87	63.38	61.18	62.33	59.97	62.24	64.42
TiO ₂	0.61	0.45	0.63	0.55	0.61	0.47	0.53	0.51	0.65	0.54	0.62	0.50	0.45
Al ₂ O ₃	17.14	15.84	16.80	17.18	16.44	16.63	17.35	16.60	17.43	17.17	17.42	17.04	16.71
Fe ₂ O ₃	4.30	3.45	5.09	3.66	4.36	2.29	3.95	4.39	4.58	3.83	4.89	4.13	2.92
FeO	0.76	1.42	0.59	1.09	1.36	1.16	0.92	0.38	0.92	0.73	1.02	0.60	1.17
MnO	0.09	0.10	0.06	0.07	0.10	0.06	0.06	0.08	0.07	0.08	0.08	0.10	0.08
MgO	2.67	1.89	2.80	2.02	2.36	1.33	1.19	1.57	1.16	1.52	1.87	1.58	1.21
CaO	5.87	4.94	5.74	4.91	5.41	4.14	4.96	4.37	5.70	5.13	5.76	4.60	4.30
Na ₂ O	4.58	3.89	4.20	4.34	3.77	4.20	4.41	3.85	4.45	4.13	4.24	4.24	4.15
K ₂ O	1.91	2.82	2.07	2.32	2.95	2.42	2.61	2.75	1.99	2.42	2.55	3.07	3.13
P ₂ O ₅	0.22	0.17	0.18	0.20	0.31	0.16	0.23	0.17	0.23	0.20	0.24	0.21	0.18
L.O.I.	2.31	1.51	1.91	1.22	1.78	1.94	1.90	1.95	1.65	1.92	1.33	1.69	1.26
Total	99.99	100.00	100.00	100.00	100.00	100.00	100.00	100.00	100.00	99.99	100.00	100.00	100.00
FeO _{tot}	4.63	4.52	5.17	4.39	5.28	3.23	4.48	4.33	5.05	4.18	5.42	4.32	3.80
<i>ppm</i>													
Ba	492					527		550	221	545		590	627
Be	0					0		0	0	0		0	0
Cr	40					10		40	30	20		0	20
Cu	57					76		44	0	53		39	45
Li	30					10		20	0	0		30	20
Mn	680					410		600	290	550		700	600
Ni	16					<5		21	28	13		8	5
Sc	7					0		7	0	6		6	0
Sr	765					636		602	364	739		670	692
V	115					82		65	61	95		79	79
Zn	76					70		65	33	83		72	74
Ag	0					0		0	0	0		0	0
As	0					0		0	0	0		0	0
Bi	0					0.2		0.3	0.2	0		0.1	0
Cd	0					0		0	0	0		0	0
Ce	58.2					38.4		61	57	58.6		87.5	82
Co	19.4					11.9		16.8	19.4	14.3		16	12.9
Cs	1.6					5.1		5.7	6.8	5.2		6	8.5
Dy	1.95					1.19		1.98	2.05	1.83		2.58	2.45
Er	1.16					0.57		1.24	1.22	1.03		1.6	1.35
Eu	1.24					0.95		1.18	1.34	1.22		1.51	1.38
Ga	21					19		18	20	20		19	19
Gd	3.43					2.2		3.16	3.55	3.26		4.33	3.85
Ge	1					1		1	1	1		1	1
Hf	3					3		4	3	4		5	5
Ho	0.4					0.22		0.41	0.43	0.37		0.54	0.51
In	0					0		0	0	0		0	0
La	39.9					25.7		41.6	37.7	39.5		60	56.3
Lu	0.14					0.1		0.16	0.16	0.14		0.22	0.19
Mo	0					0		0	0	2		0	2
Nb	8					5		8	7	7		11	10
Nd	29					19.9		27.2	28.7	28.8		38.9	36.5
Pb	9					11		17	18	12		21	22
Pr	7.88					5.24		7.76	7.86	7.98		11.2	10.5
Rb	54.2					64.9		97.4	60.5	75.3		115	113
Sb	0.5					0.4		0.7	0.4	0.6		0.7	0.7
Sm	4.9					3.2		4.3	4.9	4.6		5.8	5.6
Sn	2					1		5	2	1		2	2
Ta	0					0		0	0	0		0.6	0.5
Tb	0.45					0.31		0.45	0.51	0.46		0.64	0.54
Th	13.1					6.9		20.5	13.6	13.4		27.3	26.4
Tl	0					0		0	0	0		0.5	0.5
Tm	0.16					0.08		0.15	0.15	0.13		0.22	0.19
U	3.18					2.24		3.33	3.17	3.26		5.84	5.63
W	1					0		1	1	1		2	2
Y	11.3					6.7		12.1	12.2	11.1		16.5	14
Yb	0.9					0.5		1	0.9	0.9		1.4	1.1
Zr	111					102		146	124	131		193	181

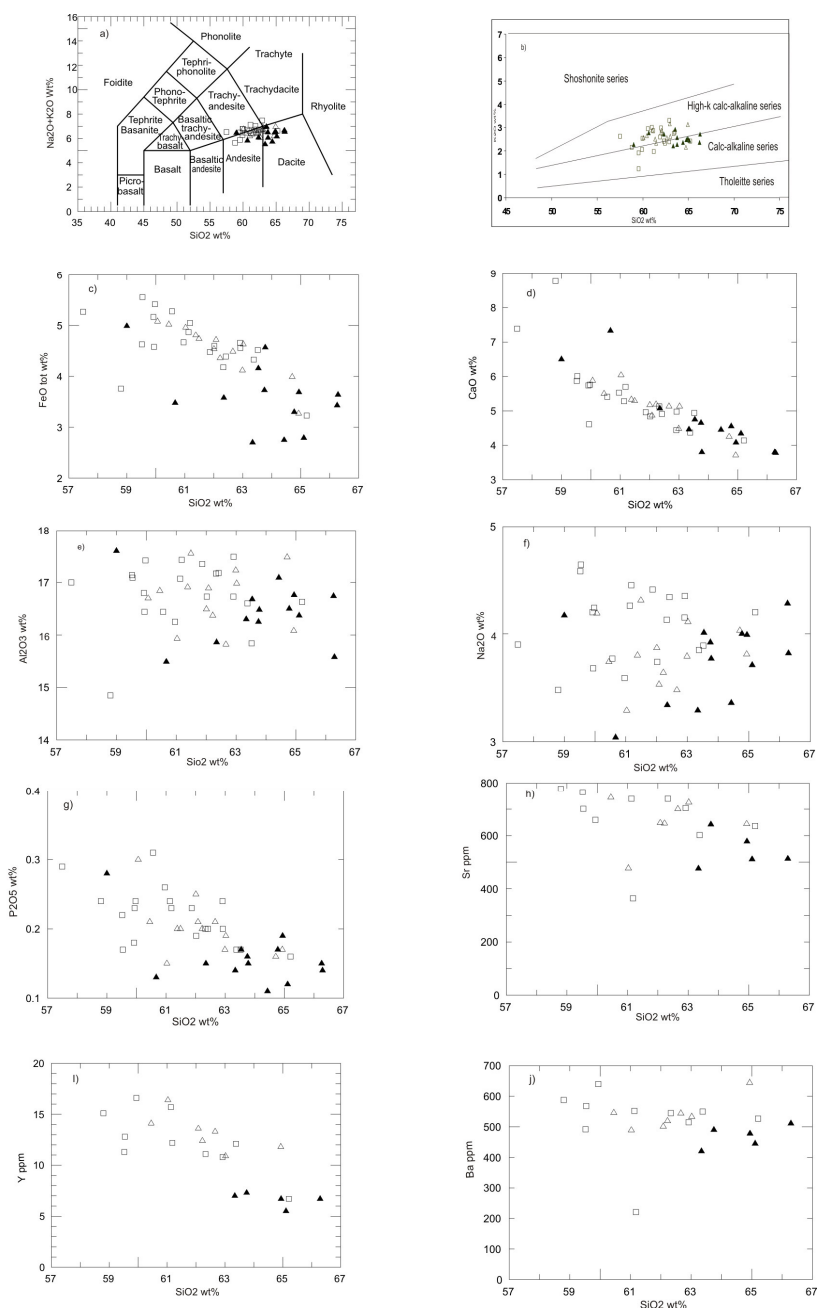


Figure 5. Whole rock major and trace element abundances of Bidkhan igneous rocks, versus SiO₂. a) Total alkali diagrams that shows classification scheme of Le bas (1983), our samples place in the field of andesite to dacite. b) K₂O versus SiO₂ classification diagram from pecerillo and Taylor (1976), majority of Bidkhan samples place in high-calc alkaline series. c-f) Major element abundances in Bidkhan rocks; g-j) Trace element abundances in Bidkhan rocks. Lithics in pyroclastic deposits (Triangle), Dykes (Dark triangles), Lava (Square).

abundant, for dacites, core with An 41-49 and for transitional rocks An 41-48 are the most. Although there

are rare cores with An 75 in andesites and some cores with An 67 in transitional rocks are present. Table 5

Table 4. Representative electron microprobe (oxides in wt%) analysis of Bidkhan plagioclase along core-rim (selected from 50 samples) An%, mol % anorthite

Sample	SiO ₂	TiO ₂	Al ₂ O ₃	FeO	MgO	CaO	Na ₂ O	K ₂ O	Total	An%
Q1(lithics of pyroclastic rocks),Plagioclase 1										
Core	61.11	0.11	24.42	0.40	0.13	5.51	7.12	0.82	99.72	28
Middle	62.25	0.13	22.74	1.08	0.26	5.62	6.30	0.98	99.63	31
Rim	58.07	0.08	26.78	0.48	0.09	7.94	5.64	0.53	99.74	42
V6(lithics of pyroclastic rocks),Plagioclase 1										
Core	49.67	0.13	32.22	0.69	0.19	14.15	2.48	0.20	99.73	75
Middle	56.52	0.12	27.38	0.53	0.12	9.08	5.39	0.43	99.73	47
Rim	58.53	0.20	25.90	0.58	0.06	7.68	5.89	0.64	99.60	40
W3(lithics of pyroclastic rocks),Plagioclase 1										
Core	53.82	0.13	29.29	0.56	0.24	11.02	4.12	0.35	99.63	58
Middle	51.77	0.14	30.77	0.68	0.22	12.28	3.26	0.26	99.47	66
Rim	59.63	0.00	25.91	0.37	0.11	7.18	6.11	0.54	99.85	38
B9(lithics of pyroclastic rocks),Plagioclase 1										
Core	57.74	0.20	25.81	1.11	0.36	7.91	5.70	0.54	99.37	42
Middle	57.34	0.00	26.98	0.53	0.26	8.93	5.47	0.33	99.84	46
Rim	71.21	0.52	15.98	1.27	0.17	2.28	4.49	3.52	99.44	16
F1(lithics of pyroclastic rocks),Plagioclase 2										
Core	54.80	0.13	27.87	0.88	0.26	10.16	4.71	0.42	99.23	53
Middle	56.80	0.15	27.14	0.40	0.30	9.25	5.20	0.47	99.71	48
Rim	53.88	0.12	29.04	0.72	0.25	10.93	4.16	0.37	99.47	58
X4(dyke),Plagioclase 1										
Core	59.50	0.12	25.27	0.52	0.18	6.52	6.62	0.67	99.40	34
Middle	60.60	0.07	25.02	0.31	0.23	6.37	6.74	0.55	99.89	33
Rim	61.51	0.23	24.16	0.34	0.16	5.57	6.86	0.76	99.59	29
Q10(dyke),Plagioclase 1										
Core	53.85	0.19	29.22	0.33	0.27	10.84	4.40	0.33	99.43	56
Middle	56.49	0.20	27.67	0.39	0.14	8.89	5.25	0.38	99.41	47
Rim	66.19	0.18	21.93	1.85	6.57	1.92	0.12	0.44	99.20	72
Q10(dyke),Plagioclase 2										
Core	59.70	0.05	25.81	0.23	0.19	7.27	6.19	0.35	99.79	38
Middle	58.47	0.07	25.93	0.38	0.20	7.69	6.06	0.38	99.18	40
Rim	58.02	0.00	26.86	0.43	0.20	8.45	5.73	0.32	100.01	44
S4(dyke),Plagioclase 1										
Core	61.49	0.11	23.93	0.39	0.18	5.61	7.07	0.68	99.46	29
Middle	61.58	0.14	23.97	0.36	0.17	5.34	7.47	0.67	99.70	27
Rim	58.85	0.18	25.74	0.36	0.20	7.53	6.19	0.50	99.55	39
D3(dyke),Plagioclase 1										
Core	57.18	0.09	27.59	0.35	0.15	9.00	5.18	0.28	99.82	48
Middle	57.69	0.17	26.83	0.30	0.07	8.36	5.55	0.40	99.37	44
Rim	59.47	0.11	25.70	0.30	0.06	7.17	6.35	0.49	99.65	37
D3(dyke),Plagioclase 2										
Core	56.27	0.22	27.59	0.47	0.24	9.34	5.07	0.32	99.52	49
Middle	56.00	0.08	27.97	0.64	0.11	9.48	5.08	0.31	99.67	50
Rim	55.68	0.10	28.23	0.55	0.25	9.66	4.84	0.31	99.62	51
T9(dyke),Plagioclase 2										
Core	56.15	0.11	27.47	0.46	0.22	9.41	5.12	0.34	99.55	49
Middle	55.71	0.24	28.10	0.39	0.27	9.69	4.89	0.31	99.75	51
Rim	55.32	0.17	28.42	0.47	0.18	10.12	4.73	0.27	99.80	53
L6(lava),Plagioclase 2										
Core	56.39	0.21	27.23	0.66	0.15	9.27	5.30	0.40	99.77	48
Middle	61.29	0.00	24.74	0.38	0.11	6.14	6.65	0.67	99.98	32
Rim	59.21	0.36	24.93	0.88	0.13	7.24	6.23	0.69	99.67	37
L6(lava),Plagioclase 3										
Core	59.19	0.09	25.69	0.59	0.28	7.69	5.78	0.62	100.01	41
Middle	57.73	0.15	26.49	0.50	0.27	8.22	5.65	0.52	99.63	43
Rim	54.19	0.10	29.02	0.68	0.24	11.03	4.58	0.33	100.28	56

Table 4. Continued

Sample	SiO ₂	TiO ₂	Al ₂ O ₃	FeO	MgO	CaO	Na ₂ O	K ₂ O	Total	An%
G7(lava),Plagioclase 3										
Core	56.91	0.15	26.91	0.56	0.34	8.45	5.65	0.61	99.76	44
Middle	58.73	0.25	25.70	0.54	0.16	7.44	5.91	0.85	99.72	39
Rim	54.08	0.06	28.65	0.72	0.12	10.95	4.43	0.44	99.68	56
I5(lava),Plagioclase 1										
Core	59.03	0.24	25.29	0.55	0.17	6.84	6.30	0.87	99.48	35
Middle	58.63	0.12	25.73	0.50	0.17	7.53	6.00	0.72	99.59	39
Core	59.25	0.22	25.17	0.60	0.08	7.06	6.18	0.81	99.55	37
T5(lava),Plagioclase 1										
Core	54.50	0.00	29.06	0.42	0.19	10.83	4.16	0.33	99.67	58
Middle	59.47	0.12	25.48	0.49	0.18	7.21	6.01	0.67	99.73	38
Rim	56.41	0.15	27.51	0.66	0.07	9.29	5.03	0.45	99.63	49
T5(lava),Plagioclase 2										
Core	55.49	0.04	28.71	0.46	0.15	10.15	4.69	0.31	100.00	53
Middle	60.21	0.19	25.09	0.50	0.00	6.33	6.52	0.77	99.71	33
Rim	64.23	0.25	21.26	1.04	0.13	3.07	6.38	3.48	99.84	16
T5(lava),Plagioclase 3										
Core	59.28	0.27	25.13	0.53	0.20	7.11	6.07	0.71	99.54	38
Middle	58.32	0.07	26.40	0.30	0.12	8.26	5.73	0.52	99.90	43
Rim	56.25	0.18	27.34	0.68	0.18	9.13	5.11	0.51	99.70	48
R7(lava),Plagioclase 1										
Core	56.34	0.15	27.71	0.65	0.12	9.34	5.05	0.27	99.71	50
Middle	57.62	0.11	26.45	0.62	0.20	8.65	5.54	0.43	99.76	45
Rim	54.57	0.12	28.37	0.78	0.29	10.39	4.48	0.34	99.56	55
C6(lava),Plagioclase 1										
Core	57.47	0.19	26.83	0.54	0.22	8.57	5.35	0.43	99.60	46
Middle	55.02	0.22	28.05	0.64	0.25	10.02	4.70	0.39	99.29	53
Rim	54.84	0.26	28.01	0.80	0.26	10.09	4.50	0.48	99.24	54
C6(lava),Plagioclase 2										
Core	56.79	0.18	27.13	0.64	0.20	8.82	5.24	0.46	99.46	47
Middle	57.47	0.00	26.88	0.50	0.20	8.78	5.35	0.39	99.57	46
Rim	55.35	0.11	27.76	0.88	0.27	9.82	4.71	0.48	99.38	52
V7(lava),Plagioclase 2										
Core	56.94	0.25	26.88	0.57	0.10	8.88	5.24	0.53	99.39	47
Middle	58.65	0.11	26.23	0.38	0.30	7.63	5.70	0.66	99.66	41
Rim	58.99	0.15	25.87	0.46	0.21	7.35	6.02	0.71	99.76	39
N1(lava),Plagioclase 1										
Core	58.43	0.19	25.81	0.54	0.20	7.33	6.04	0.80	99.57	38
Middle	59.38	0.18	25.31	0.46	0.14	6.66	6.26	0.97	99.49	35
Rim	58.78	0.16	25.73	0.40	0.20	7.70	6.13	0.58	99.86	40
N1(lava),Plagioclase 2										
Core	61.86	0.20	20.43	1.40	1.50	7.06	4.77	1.97	99.68	39
Middle	56.11	0.14	27.38	0.55	0.23	9.62	4.94	0.58	99.75	50
Rim	59.59	0.24	25.00	0.56	0.20	6.96	6.42	0.56	99.60	36
An(lava),Plagioclase 1										
Core	52.04	0.13	30.25	0.53	0.24	12.33	3.28	0.33	99.13	66
Middle	58.65	0.28	25.75	0.65	0.24	7.49	5.74	0.69	99.49	40
Rim	65.64	0.18	20.18	0.73	0.18	2.08	6.25	4.43	99.67	11
An(lava),Plagioclase 2										
Core	56.78	0.24	27.08	0.52	0.15	8.90	5.09	0.59	99.35	47
Middle	60.51	0.17	24.59	0.44	0.28	6.27	6.45	0.88	99.59	33
Rim	61.83	0.19	23.98	0.56	0.00	5.32	6.69	1.06	99.63	28
P1(lava),Plagioclase 2										
Core	61.34	0.10	24.32	0.32	0.13	5.85	6.70	0.78	99.54	31
Middle	59.83	0.14	25.21	0.34	0.17	6.84	6.34	0.72	99.59	36
Rim	54.35	0.15	28.99	0.53	0.13	10.85	4.30	0.31	99.61	57

indicates that certain plagioclase crystals are not belong to the specific rock types, moreover, there are several plagioclase generations with various compositions in each rock type. Composition profiles from core to rim for some plagioclase grains are shown in Figure 7. Clearly, there are compositional variations in plagioclase crystals that reflect their complex history. Detailed studies in these profiles revealed that in Bidkhan rocks, many plagioclase crystals are compositional zoned and four types of zonation were distinguished in our plagioclase (Fig. 8).

1) Normal zoned plagioclases that occur throughout the compositional spectrum of Bidkhan rocks (Fig. 8). In this type, An mol% varies from 53 in core to 10 in the rim, and crystals have not any internal dissolution surfaces (Fig. 8); thus, they reflect near equilibrium growth from a melt progressively depleted in the components crystallizing. 2) Reversely zoned plagioclase crystals that make up a significant percentage of the Bidkhan plagioclases and occur in all of the rock types (Fig. 8), with a compositional range from 30 An mol% in core to 55 in rim. 3) Normal oscillatory zoned plagioclases that also occur in all of the rock types (Fig. 8); their An mol% fluctuates from core to rim, but in the rim (An 30) is much more than the core (An 54). This type has interpreted as evidence of repeatedly entrance of newly batches of magma into the chamber. The Δ An in oscillations are relatively small (~ 5 An mol%), that suggest newly melts were nearly similar in composition. 4) Reverse oscillatory zoned plagioclases occur in three types of the Bidkhan rocks (Fig. 8). In this group of plagioclase crystals, An content fluctuates (with Δ An ~ 10 mol %) and increases from their core to rim overall. These types of plagioclases are shown in Figure 8 to find chemical evolution of them during magmatic events.

Investigation of chemistry data in Bidkhan reveals that there are some plagioclase crystals with calcic cores (An 75 mol%) in andesites. Experimental works on equilibrium crystallization in magma systems, show that in andesitic magmas, the An content of plagioclase would not exceed 48-52 mol% An at pressure of 0.1-200 mpas, temperature of 800-1300 °C and water content of 0-4 wt% [3]. This composition is agreement with the core of some plagioclase phenocrysts in Bidkhan andesites (Sample V6), but in andesites we have plagioclases with An mol% 75 in the core and according to the experiments [3] plagioclases as calcic as An 76-90 can not crystallize in equilibrium with andesitic melt at any pressure, temperature and water content and thus this type of plagioclase phenocryst must have introduced to the Bidkhan andesites from a more mafic source. The coarse sieved interior of some

An rich plagioclase phenocrysts (Fig. 7c) indicates that the cores were subjected to the process of dissolution prior to entrance in shallow magma chamber probably due to decompression of ascending host melts [22].

There are several zonation patterns in plagioclase phenocrysts from the same rock. Some crystals show normal zoning (Fig. 8), some show reverse and some of them are oscillatory zoned. These features must be established due to magma mixing. In general, the range of core compositions of plagioclases in Bidkhan is An 55, larger than that of their rim's composition (An 20). This situation that has stated by Toothil [34], means a combination of fractionation and magma mixing, where crystals growth in a relatively shallow magma chamber has periodically been interrupted by injection of other melts, with nearly similar composition.

Table 5. An mol% ranges in the core of plagioclase phenocrysts of Bidkhan different rocks

Name of rock	Number of samples			
	An mol% more than 60	An mol% between 50-60	An mol% between 40-50	An mol% less than 40
Andesites	1 (75)	5 (50-56)	1 (40)	4 (35-38)
Dacites		2 (52-58)	5 (41-49)	4 (28-34)
Transitional rocks between Andesites and Dacites	2 (61-67)	6 (50-58)	12 (41-48)	6 (30-39)

Numbers in parentheses are the An% and their ranges

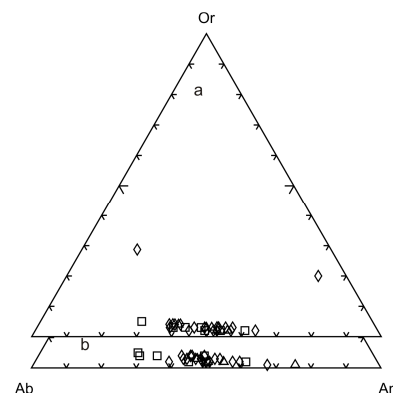


Figure 6. The compositions of plagioclase phenocryst rims (a) and cores (b) plotted on An-Ab-Or diagram. In general, cores are slightly more calcic than the rims. Andesites (Triangle), Dacites (square), Transitional (Diamond).

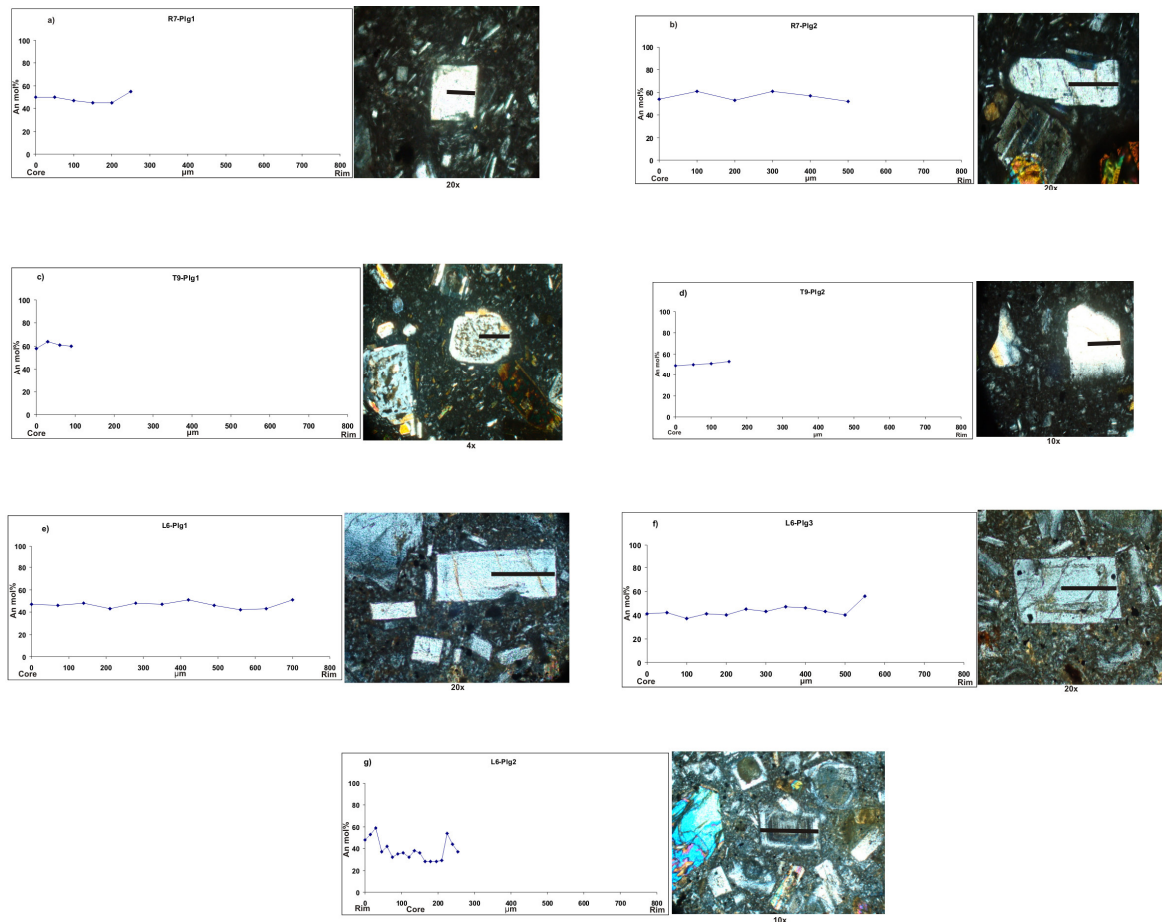


Figure 7. Photomicrographs of different populations of plagioclase crystals from Bidkhan eruptive products, and mol% An along core to rim sampling transects (a-f); g) A traverse across an oscillatory zoned plagioclase phenocryst. Solid lines in photos indicate path of transect for electron microprobe analysis.

Many plagioclase phenocrysts have thin more sodic rims (Fig. 7), which have similar An content (An 20) to plagioclase microlites in the matrix. These are probably crystallized during eruption. The An rich rims on the reversely zoned plagioclase phenocrysts may be associated with the last hybridization events that occur in shallow magma chamber.

Finally evidence such as the wide range of plagioclase core composition in individual rocks, the lack of clear correlation between plagioclase and host rock compositions, the occurrence of reverse zoning in plagioclases and occurrence of xenocrystic plagioclase indicate that magma mixing have played roles in magmatic evolution.

Magma Mixing

Almost all of criteria for identification of magma mixing in silicic-intermediate rocks, such as disequilibrium textures, occurrence of normally and reversely zoned plagioclase in the same sample [14], occurrence of unusual mineral composition [23], and occurrence of heterogeneous plagioclase core and rim composition [37], exist in Bidkhan eruptive products.

Study of disequilibrium textures and variation of mineral composition has been the most effective way of fingerprinting the role of magma mixing in intermediate rocks. In the light of these evidences, we found that there are two distinctive magma mixing events in Bidkhan parent magmas. It is probably that The first

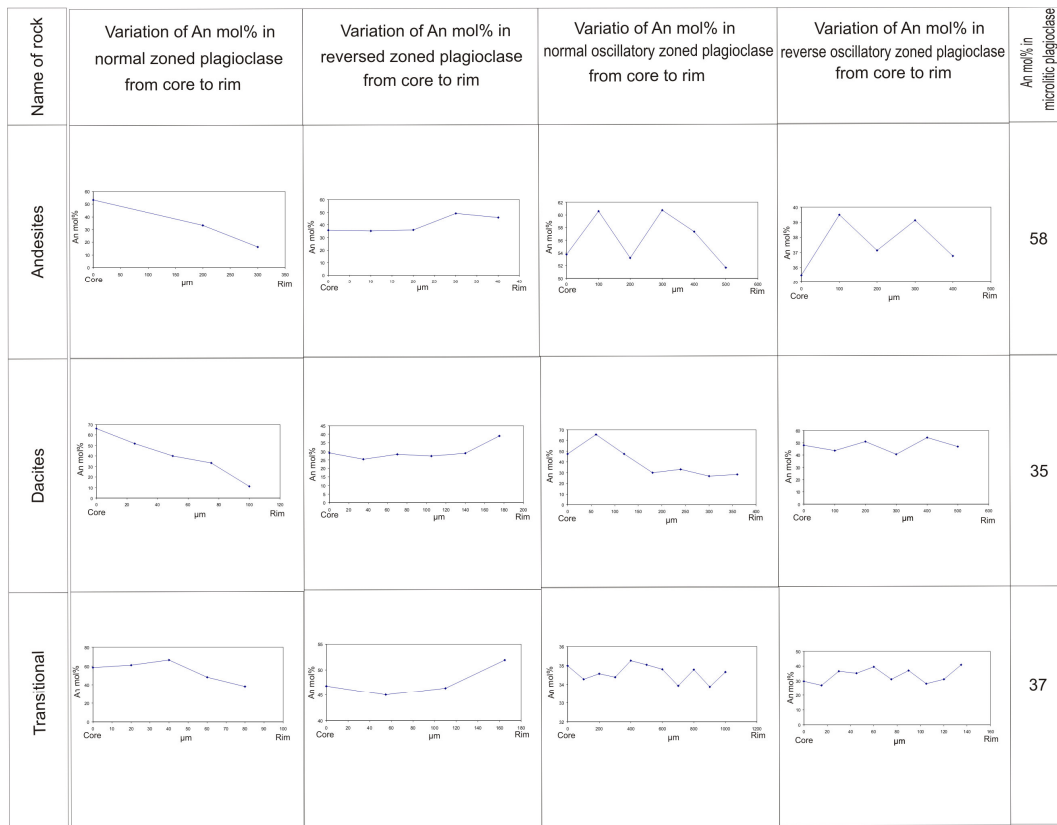


Figure 8. Compositionally various types of plagioclase in Bidkhan rocks and their compositional variation patterns from core to rim.

mixing events have occurred in great depths of the crust, between basic (probably basaltic or basaltic andesite) and acidic (probably dacitic) melts. This event happened prior to entrance of hybrid magmas into the shallow magma chambers. For this reason, nowadays we have not any eruptive product from these original melts in Bidkhan, but xenocrystic inherited plagioclase cores that are not in equilibrium with their host rocks, suggest that these melts could have been existed. There are some calcic-cored plagioclases (An 75) with more sodic rims (An 40) in andesites; also there are sodic-cored plagioclases (An 28) with more calcic rims (An 42) in these rocks (Table 2). The first plagioclases can be inherited from a basaltic melt [3], whereas the second ones may become from a dacitic melt and then, both minerals have placed in an intermediate hybridized melt to form rims with similar compositions (An 40 and An 42).

Second mixing event occurs in the shallow magma chamber between hybridized intermediate magmas with nearly similar composition. For this reason, the compositional range of Bidkhan eruptive products is

from andesite to dacite, moreover, the composition of irregular bands in mingled rocks are nearly similar and both mingled melts show many similar features for magma mixing.

Results and Discussion

There are many evidence show that rock associations in Bidkhan stratovolcano have been produced from magmas representing different magma mixing and crustal assimilation processes. But there is not any direct evidence from original end-member melts, and all of the erupted magmas have intermediate to acidic composition. So these melts have earned their relationships in the shallow magma chambers. In other word, after mixing of original magmas (basaltic and dacitic melts) in deep of the crust, resulted hybridized melts ascend toward shallow depths and produce Bidkhan eruptive magmas.

Because this part of central Iranian continental crust is relatively thick [6], [1], it is probable that mantle derived basic magmas are stopped in the lowermost part

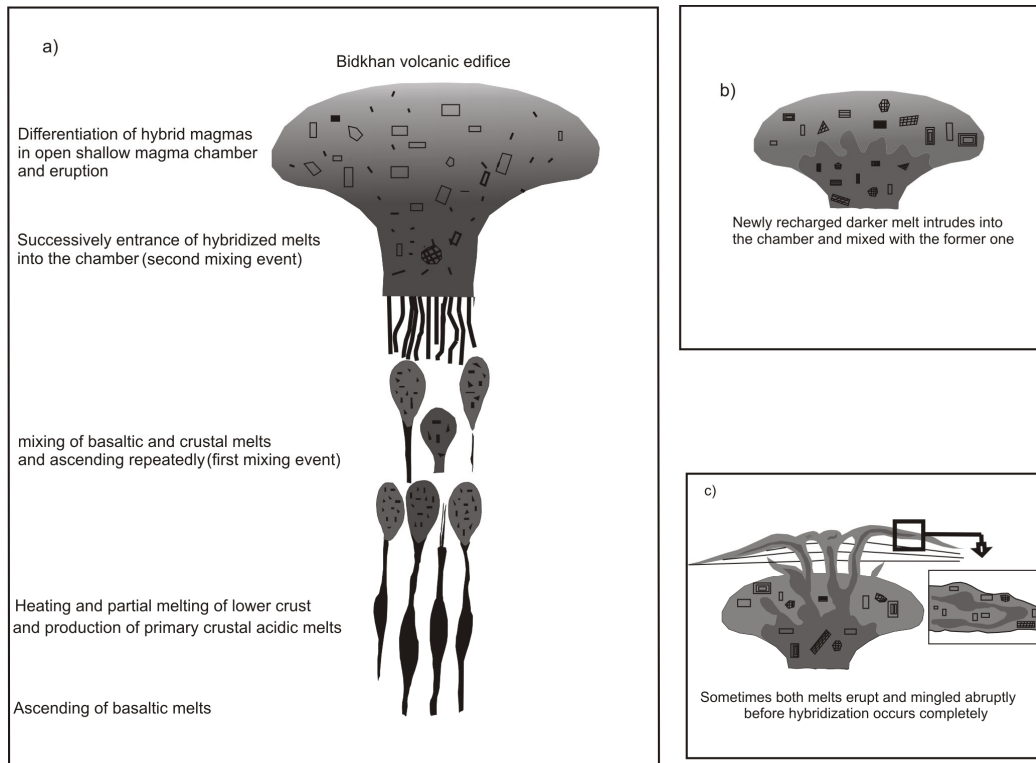


Figure 9. Schematic model for the evolution of Bidkhan parent magmas based on whole evidence. a) Injection of mantle derived basic magmas and partial melting of lower crust, generation of primitive acidic melts and mixing of two magmas to form hybrid intermediate melts. Ascending hybrid melts toward shallow reservoirs and repeatedly injection of these melts cause mixing, differentiation and eruption of andesitic to dacitic magma of Bidkhan volcano.

of the crust and begin to crystallize. These magmas can cause partial melting events in lower crust and acidic original melts are produced. Then, these melts mix and the first mixing event occurs in this situation, and intermediate hybridized melts are formed. Nowadays, we have just some records from original melts in Clinopyroxene and plagioclase phenocrysts. Al and Ti rich clinopyroxenes associated with calcic cored sieved plagioclases in andesitic rocks are inherited xenocrysts that have been formed in a basic melt. Then, these plagioclases have placed in intermediate hybridized magmas to form zoned and oscillatory rims (with An 75) around calcic cores. On the other hand, in the same rock, there are more sodic cored plagioclase phenocrysts (An 40) that could have crystallized in more silicic melts (more silicic than andesite). These crystals also have oscillatory and reversely zoned rims (Fig. 4) similar in composition to the former plagioclase rims.

This means that the cores of these two types of plagioclases have been crystallized in separated melts (probably in original basic and acidic melts) and then,

they have placed in the same hybridized melts and their similar rims formed simultaneously in new magma. Sieved and dusty textures are commonly reported in igneous rocks of proposed magma mixing origin [36]. These textures also form due to decompression, when magma rises toward the surface [22].

In this case, there should not be any compositional changes accompanying the corrosion of the crystals [19]. Moreover, if sieved plagioclases were formed due to mixing, there should be some kinds of compositional changes, like the case of Bidkhan rocks (Fig. 4).

All of evidence shows that in Bidkhan, hybridized melts ascend and emplace in shallow magma chambers. The chambers are open system and repeatedly invaded by intermediate hybridized melts and second magma mixing event have occurred in this situation. The composition of these melts can be changed depends on the amount of acidic and basic original end member magmas. When a newly batch of magma enters into the chamber, whole composition of magma changes and another rim is formed on the former plagioclase core,

and gradually, oscillatory zoned plagioclase (Fig. 4) are produced. Some xenocrystic calcic plagioclases in this case, are resorbed to form sieved or dusty textured crystals (Fig. 4). In Shallow chambers, there have been enough time for differentiation, so a range of magmas from andesite to dacite formed due to fractional crystallization of hybridized magma.

Because these magmas are intermediate, the compositional spectrum of their differentiation controlled by crystallization of pyroxenes, plagioclase and amphibole. So in these magma chambers some of plagioclases phenocrysts have totally equilibrated with the host melts (Fig. 4), but there are some xenocrystic plagioclases in these melts that have involved into new stage of crystallization and oscillatory or reversed zoned rims formed around the former cores (Fig. 4).

The heat come from new batches of magma cause establishment of convection cells and phenocrysts are suspended in the magma. As a result, during eruption we can see a variety of phenocrysts in eruptive products. At the time of eruption, a clear thin rim is formed around the former plagioclases with composition similar to groundmass plagioclase microlites (Fig. 4).

Eruptive melts range from dacitic to andesitic in composition and sometimes, two melts erupted in the same time as mingled magmas, before mixing event completely occur in the chamber (Fig. 9).

Based on field, petrography and chemistry evidence, we propose a multi-stage model for magmatic evolution of Bidkhan (Fig. 9). The stages of the model are as follows:

1) Original mantle derived basic melts cause partial melting of lower crust and mixed with acidic resultant melts, and intermediate hybridized magma are formed.

2) Newly formed magmas ascend to shallow chambers, crystallize and fractionate and mineral assemblages dominant by plagioclases are produced.

3) Repeated injections of hybridized magmas into the chamber caused second mixing event and formation of oscillatory and reverse zoning in the former phenocrysts.

4) Eruption of andesitic to dacitic magmas. Sometimes two melts erupted as mingled melts.

In Bidkhan stratovolcano, there are many petrological evidences that demonstrate magma mixing is a principal process for the origin of the textural and mineralogical characteristic of the rocks. Detailed studies show that this process has been done in different stages and situations. This means that Bidkhan lavas and pyroclastics can not produced by simple two component magma mixing. Indeed, these products have been formed by several mixing of hybridized intermediate melts with nearly similar compositions.

Hybrid melts, in turn, can be tested for other igneous provinces in central Iranian volcanic belt.

Acknowledgement

The authors wish to thank professor A. Aftabi, A. Moradian, M. viccaro and R. crisofolini for critical discussions and their helps.

References

1. Alavi, M. Tectonic of the zagros orogenic belt of Iran: new data and interpretations. *Tectonophysics.*, **229**: 211-238 (1994).
2. Anderson, U.B., Eklund, D. Cellular plagioclase intergrowths as a result of crystal-magma mixing in the proterozoic aland rapakivi batholith Sw finland. *contrib. mineral. petrol.*, **117**: 124-136 (1994).
3. Ariskin, A.A. Phase equilibria modeling in igneous petrology: Use of COMAGMAT model for simulating fractionation of ferro basaltic magmas and the genesis of high alumina basalt. *J. Volcanol. Geotherm. Res.*, **90**:115-162 (1999).
4. Bacon, C.R. Magmatic inclusions in silicic and intermediate volcanic rocks. *Journal of geophysical research.*, **91**: 6091-6112 (1986).
5. Browne, B.L., Eichelberger, J.C., Patino, L.C., Vogel, T.A., Dehn, J., Uto, K., Hoshizumi, H. Generation of porphyritic and equigranular mafic Enclaves during magma recharge events at Unzen volcano, Japan. *J. Petrol.*, **47**(2): 301-328 (2006).
6. Dehghani, G.A., Makris, j. The gravity field and crustal structure of Iran, in geodynamic project(geotravers)in Iran. *Geol. surv. iran, rep.*, No 51: 51-68 (1983).
7. Dimitrijivic, M.D. Geology of kerman region, geological survey of Iran. *Rep.*, **No yu/52**: 334p (1973).
8. Eichelberger, J.C., Izbekov, P.E. Eruption of andesite triggered by dyke injection: contrasting cases at karymsky volcano, kamchatka and Mt katmai, Alaska . *Phil. Trans. R. Soc. Lond.*, **358**: 1465-1485 (2000).
9. Emami, M.H., Michel, R. Observation petrographique d'un can de mélange des magmas acid et basique: genese des dacitoides de la region de Qom-aran(Iran central). *Bull. Volcanol.*, **vol 47-4 No 1**: 769-779 (1984).
10. Feeley, T.C., Dungan, M.A. Compositional and dynamic controls on mafic-silicic magma interactions at continental arc volcanoes: evidence from cardon El Guadal, Tatara, san pedro complex, chile. *J. Petrol.*, **37**: 1547-1577 (1996).
11. Feeley, T.C., Cosca, M.A. Lindsay, C.R. Petrogenesis and implications of calc-alkaline cryptic hybrid magmas from Washburn volcano, Absaroka volcanic province, USA. *J. Petrol.*, **43**(4): 663-703(2002).
12. Foden, J.D., Green, D.H. Possible role of amphibole in the origin of andesite: some experimental and natural evidence. *Contrib. Mineral. Petrol.* **109**: 479-493 (1992).
13. Franzini, M., Leoni, L., Saitta, M., A simple method to evaluate the matrix effect in x-ray fluorescence analysis. *X-ray spectrum.*, **1**: 151-154 (1972).

14. Halsor, S.P., and Rose, W.I. Mineralogical relations and magma mixing in calc alkaline andesites from lake Atitlan, Guatemala. *Mineral. Petrol.*, **45**: 47-64 (1994).
15. Humphreys, M.C.S., Blundy, J.D., Sparks, R.S.J. Magma evolution and open system processes at Shiveluch volcano: insights from phenocryst zoning. *J. Petrol.*, **47(12)**: 2303-2334 (2006).
16. Hassanzadeh, J. Metallogenic and tectonomagmatic events in the SE sector of the Cenozoic active continental margin of central Iran (Shahr-e-Babak area Kerman province). Thesis, University of California, Los angeles, (1993).
17. Izbekov, P.e., Eichelberger, J.C., Patino, L.C., Vogel, T.A., Ivanov, B.V. calcic cores of plagioclase phenocrysts in andesite from Karymsky volcano: evidence for rapid introduction by basaltic replenishment. *Geology.*, **30(9)**: 799-802 (2003).
18. Kratzmann, D., Carey, S., Scasso, R., Naranjo, J.A. Compositional variations and magma mixing in the 1991 eruption of Hudson volcano, Chile. *Bull. Volcanol.*, **71(4)**: 419-439 (2009).
19. Kuscu, G.G., Floyd, P.A. Mineral compositional and textural evidence for magma mingling the Saraykent volcanics. *Lithos.*, **56(2-3)**: 207-230 (2001).
20. Le maitre, R. W., Bateman, P., Dudek, A., Keller, J., Lemeyer, J., Le Bas, M. J., Sabine, P. A., Schmid, R., Sorensen, H., Streckeisen, A., Wooley, A. R. and Zanettin, B. A classification of igneous rocks and glossary of terms. Oxford: Blackwell., (1989).
21. Macdonald, R., Belkin, H.E., Fitton, J.G., Rogers, N.W., Nejbort, K., Tindle, A.G., Marshal, A.S. The role of fractional crystallization, magma mixing, crystal mush remobilization and volatile-melt interactions in the genesis of young basalt-peralkaline rhyolite suite, the Greater Olkaria Volcanic Complex, Kenya Rift Valley. *J. Petrol.*, **49**: 1515-1547 (2008).
22. Martel, C., radali ali, A., Poussineau, s., Gourgard, a., pichavant, M. Basalt-inherited microlites in silicic magmas: evidence from mount Plee'(Martinique, French West Insides). *Geology.*, **34 (11)**: 905-908 (2006).
23. Nakada, S., Shimizu, H. and Ohata, K. Overview of the 1990-1995 eruption at Unzen. *J. Volcanol. Geotherm. Res.*, **89**: 1-22 (1999).
24. Nelson, S.T., Montana, A., 1992. sieved textured plagioclase in volcanic rocks produced by rapid decompression. *Am. Mineral.* **72**, 1242-1249.
25. Pearce, T.H., kolisnik, A.m. Oservation of plagioclase zoning using interference imaging. *Earth Science Reviews.*, **29**: 9-26 (1990).
26. Pecerillo, A., Taylor, S.R. Geochemistry of Eocene calc-alkaline volcanic rocks from the Kastamonu area Northern Turkey. *Contrib. Mineral. Petrol.*, **58**: 63-81 (1976).
27. Shahabpour, J. Island arc affinity of the Central Iranian Volcanic Belt. *Journal of Asian Earth Sciences.*, **30**: 625-665 (2007).
28. Shahabpour, J. Tectonic evolution of the orogenic belt located between Kerman and Neyriz. *Journal of Asian Earth Sciences.*, **24**: 405-417 (2005).
29. Soheili, M. Geological map of Sirjan (1:250000). Geological survey of Iran., **map No I 11**: (1995).
30. Snyder, D., Tait, s. Magma mixing by convective entrainment. *Nature.*, **379**: 529-531 (1996).
31. Sparks, R.S.J., Sigurdsson, H., Wilson, L. Magma mixing: a mechanism for triggering acid explosive eruption. *Nature.*, **267**: 315-318 (1977).
32. Sparks, R.S.J., Marshal, L.A. Thermal and mechanical constraints on mixing between mafic and silicic magmas. *J. Volcanol. Geotherm. Res.*, **29**: 99-124 (1986).
33. Tepley, F.J.III, Davidson, J.P., Tilling, R.I., Arth, J.G. Magma mixing, recharge and eruption histories recorded in plagioclase phenocrysts from El chichon volcano, mexico. *J. Petrol.*, **41 (9)**: 1379-1411 (2000).
34. Toothill, J., Williams, C.A., Macdonald, R., Turner, S.P., Rogers, N.W., Hawkesworth, C.J., Jerman, D.A., Ottley, C.J., Tindle, A.G. A complex petrogenesis for an arc magmatic suite, St Kitts, Lesser Antilles. *J. Petrol.*, **48 (1)**: 3-42 (2007).
35. Troll, V.R., Schmincke, H.U. Magma mixing and crustal recycling recorded in ternary feldspar from compositionally zoned peralkaline ignimbrite 'A', Gran canaria, Canary Islands. *J. Petrol.*, **43(2)**: 243-270 (2002).
36. Tsuchiyama, A. Dissolution kinetics of plagioclase in the melt of the system diopside-albite-anorthite, and origin of dusty plagioclase in andesites. *Contrib. Mineral. Petrol.*, **89**: 1-16 (1985).
37. Wallace, P.J., Carmichael, I.S.E. Petrology of volcan tequila, jalisco, mexico: disequilibrium phenocryst assemblages and evolution of the subvolcanic magma system. *Contrib. Mineral. Petrol.*, **117**: 345-361 (1994).